

## Supporting Information

# Unsubstituted Thiophene-Diketopyrrolopyrrole Conjugated Polymer Thin Films via Oxidative Chemical Vapor Deposition - Electronic Behavior

*Marek K. Charyton,<sup>1</sup> Tobias Reiker,<sup>2,3</sup> Kamil Kotwica,<sup>4,5</sup> Monika Góra,<sup>6</sup> Helmut Zacharias,<sup>2</sup>  
and Nicolas D. Boscher<sup>1,\*</sup>*

<sup>1</sup> Materials Research and Technology Department, Luxembourg Institute of Science and Technology, L-4362 Esch-sur-Alzette, Luxembourg.

<sup>2</sup> Center for Soft Nanoscience, University of Münster, Münster 48149, Germany.

<sup>3</sup> Physics Institute, University of Münster, Münster 48149, Germany.

<sup>4</sup> Faculty of Chemistry, Warsaw University of Technology, 00-664 Warszawa, Poland

<sup>5</sup> Institute of Physical Chemistry, Polish Academy of Sciences, 01-224 Warszawa, Poland

<sup>6</sup> Faculty of Chemistry, University of Warsaw, 02-093 Warszawa, Poland

\* To whom correspondence should be addressed:

N. D. Boscher (email: [nicolas.boscher@list.lu](mailto:nicolas.boscher@list.lu))

**Table S1.** Deposition conditions, amounts of sublimed reactants and conductivity of the reference sublimed **sTDPP** and **sBEHTDPP** coatings and oCVD **pTDPP** and **pBEHTDPP** coatings prepared from the sublimation or oCVD reaction of 3,6-di(2-thienyl)-2,5-dihydropyrrolo[3,4-c]pyrrole-1,4-dione (TDPP) or 2,5-bis(2-ethylhexyl)- 3,6-di(2-thienyl)-2,5-dihydropyrrolo[3,4-c]pyrrole-1,4-dione (BEHTDPP), respectively.

Name	sTDPP	pTDPP	pBEHTDPP	sBEHTDPP
Monomer	TDPP		BEHTDPP	
Chemical formula	$C_{14}H_8N_2O_2S_2$		$C_{30}H_{40}N_2O_2S_2$	
Molecular weight	$300.36 \text{ g}\cdot\text{mol}^{-1}$		$524.78 \text{ g}\cdot\text{mol}^{-1}$	
Sublimation temperature	$255^\circ\text{C}$		$155^\circ\text{C}$	
Sublimed amount	$12.9 \pm 1.8 \text{ mg}$ $43.0 \pm 6.0 \mu\text{mol}$		$23.6 \pm 4.5 \text{ mg}$ $47.8 \pm 9.0 \mu\text{mol}$	
Oxidant	N/A	$\text{FeCl}_3$		N/A
Molecular weight		$162.20 \text{ g}\cdot\text{mol}^{-1}$		
Sublimation temperature		$170^\circ\text{C}$		
Sublimed amount		$308 \pm 46 \text{ mg}$ $1915 \pm 286 \mu\text{mol}$		
Conductivity	$7.8 \cdot 10^{-10} \text{ S}\cdot\text{cm}^{-1}$	$1.7 \cdot 10^{-3} \text{ S}\cdot\text{cm}^{-1}$	$9.7 \cdot 10^{-5} \text{ S}\cdot\text{cm}^{-1}$	$1.3 \cdot 10^{-10} \text{ S}\cdot\text{cm}^{-1}$
Surface roughness (Sa)	$1.8 \pm 0.2 \text{ nm}$	$2.3 \pm 0.3 \text{ nm}$	$10.7 \pm 0.3 \text{ nm}$	$1.4 \pm 0.1 \text{ nm}$

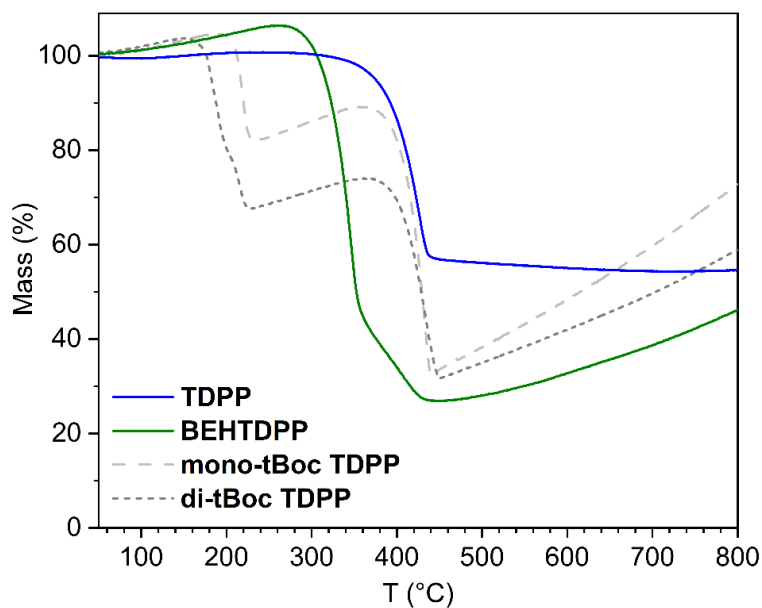
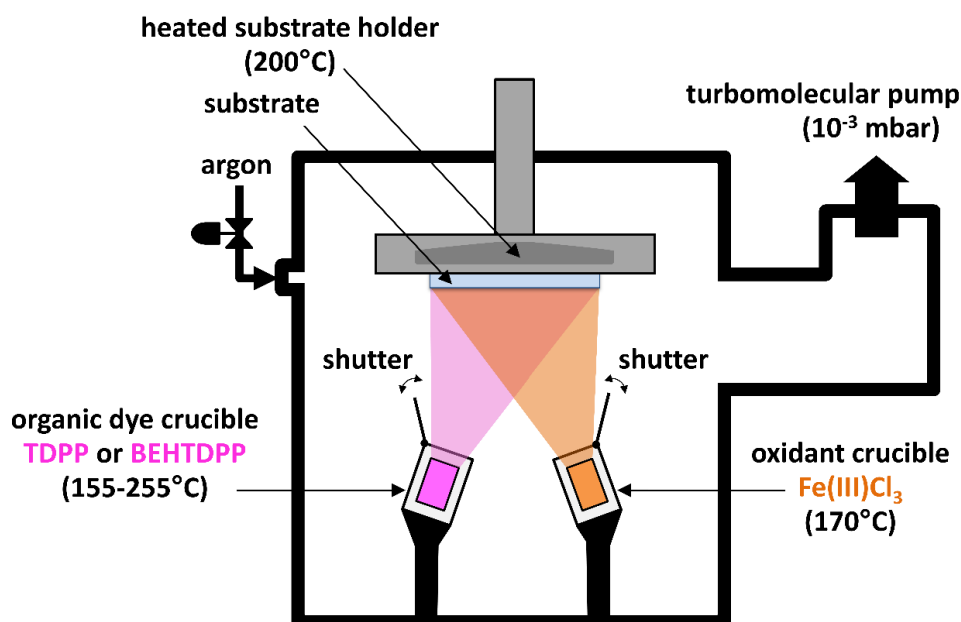


**Figure S1.** Thermogravimetric analysis of the investigated TDPP monomers. The TDPP and BEHTDPP monomers exhibit a good thermal stability in the range of temperature used during the oCVD process.



**Scheme S1.** Schematic of the custom-built oCVD reactor used for the preparation of the TDPP and BEHTDPP-based conjugated polymer thin films. Two crucibles, placed at the bottom of the oCVD chamber and oriented upward towards the heated substrate holder (200°C), are used to sublime the TDPP and BEHTDPP monomers (155-255°C) and the oxidant (170°C).

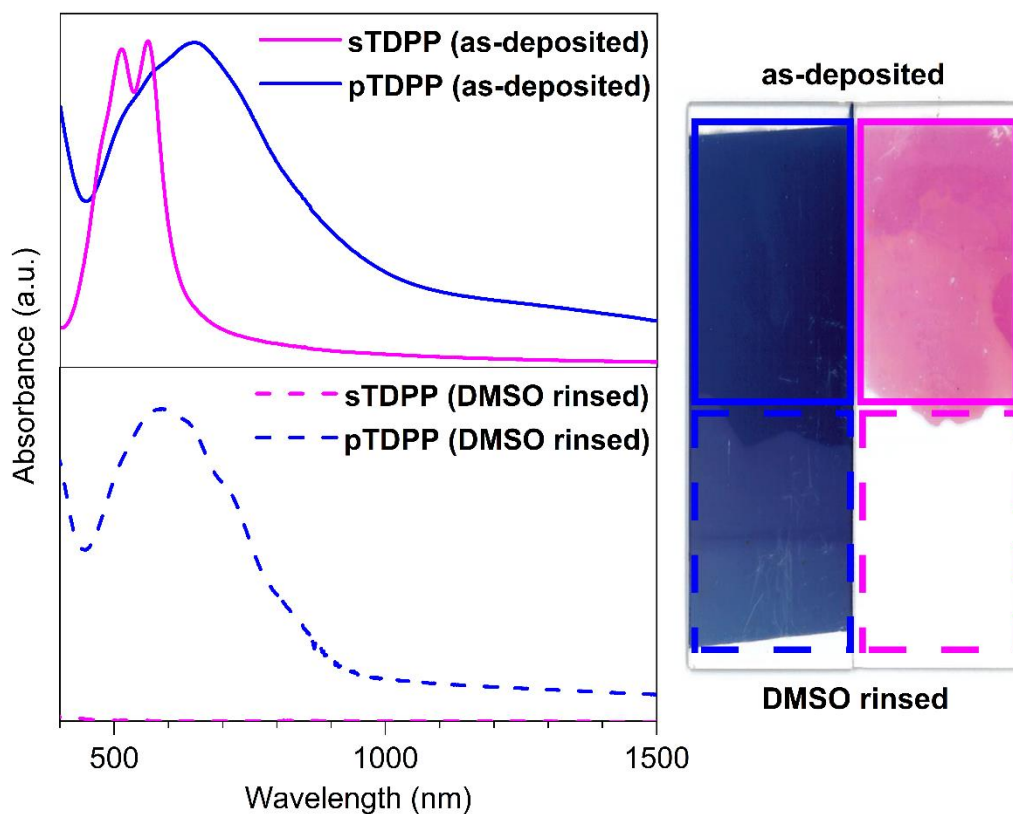


**Figure S2.** UV/Vis/NIR spectra and optical images of as-deposited **sTDPP** and **pTDPP** coatings (solid lines) and DMSO rinsed **sTDPP** and **pTDPP** coatings (dashed lines).

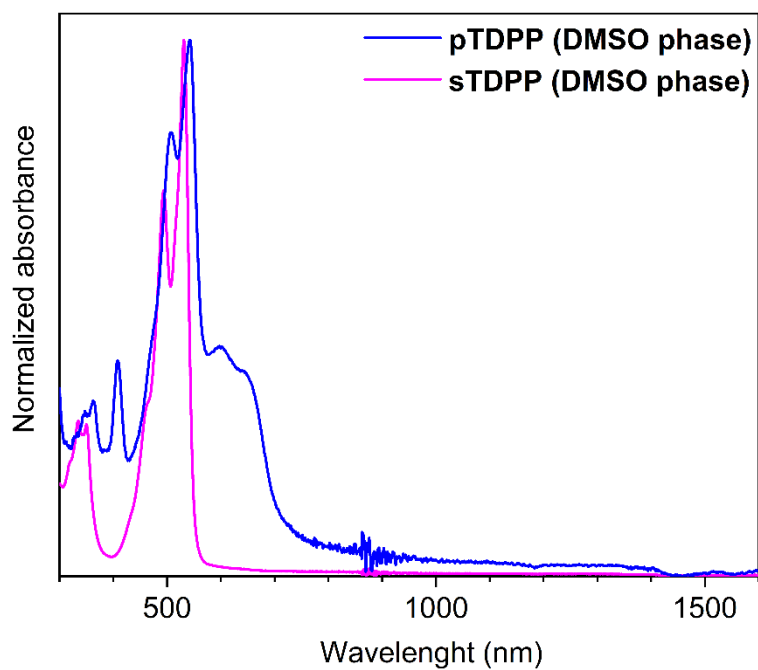


**Figure S3.** UV/Vis/NIR spectra of the soluble phase of the **sTDPP** and **pTDPP** coatings in DMSO.

**Table S2.** Relative atomic concentration determined by XPS for the sublimed **sTDPP** and oCVD **pTDPP** coatings and theoretical composition of TDPP monomer and TDPP oligomers.

	C (at.%)	N (at.%)	O (at.%)	S (at.%)	Cl (at.%)	Fe (at.%)
TDPP & TDPP <sub>n</sub> theo.	70.0	10.0	10.0	10.0	0.0	0.0
<b>sTDPP</b>	72.4	8.4	9.8	9.3	0.0	0.0
<b>pTDPP</b>	51.9	2.5	23.8	2.2	6.1	13.4

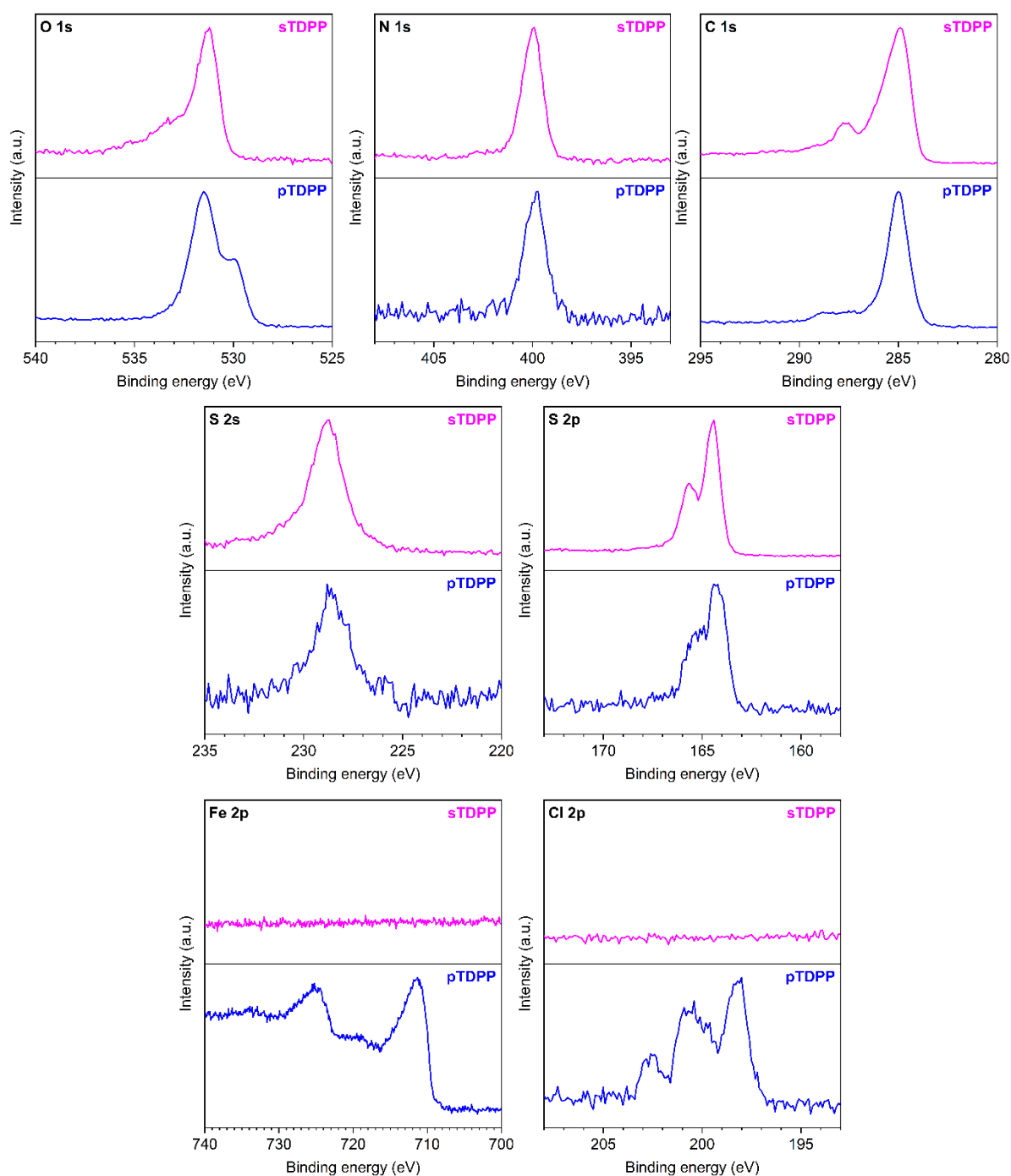
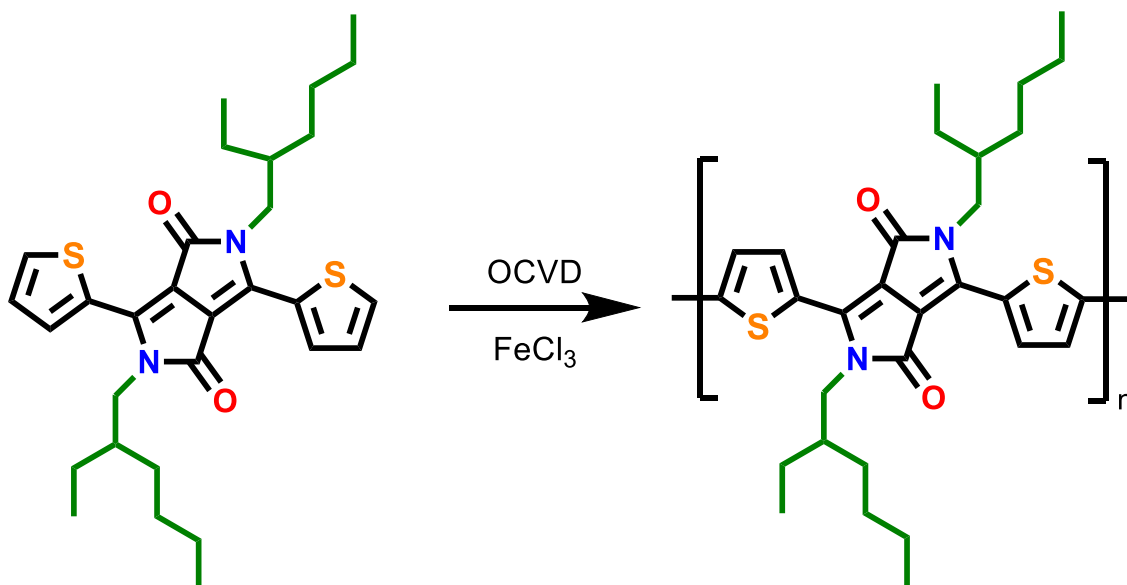


**Figure S4.** XPS spectra of the O 1s, N 1s, C 1s, S 2s, S 2p, Fe 2p and Cl 2p core levels for the sublimed **sTDPP** coating (pink) and oCVD **pTDPP** coating (blue). The Cl 2p core level XPS spectrum of **pTDPP** reveals the presence of two chlorine environments associated to the metal chloride environment (Cl 2p<sub>3/2</sub> = 198.2 eV and Cl 2p<sub>1/2</sub> = 199.8 eV) related to the presence of unreacted FeCl<sub>3</sub> or FeCl<sub>2</sub> by-products and to organic chloride (Cl 2p<sub>3/2</sub> = 200.8 eV and Cl 2p<sub>1/2</sub> = 202.5 eV) related to the chlorination of the TDPP.



**Scheme S2.** Molecular structures of BEHTDPP (left) and the conjugated polymer (right) formed from the oxidative intermolecular coupling reaction of BEHTDPP in the presence of  $\text{FeCl}_3$ . Due to the alkyl groups attached at the axial positions of TDPP motif, hydrogen bonds between BEHTDPP monomers, oligomers and polymer chains are not allowed and strongly hinder  $\pi$ - $\pi$  intermolecular interactions.

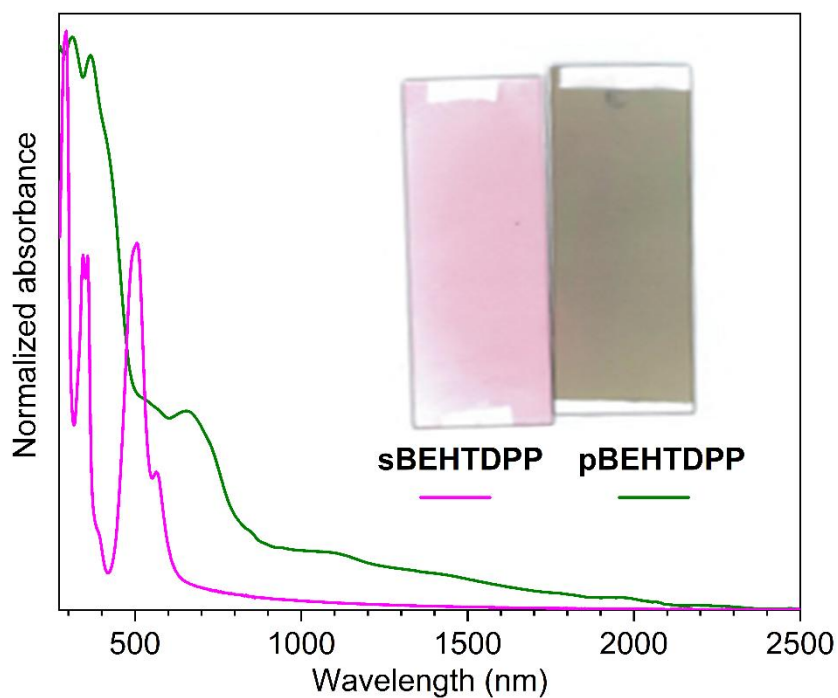


**Figure S5.** a) Optical images (inset) and UV/Vis/NIR spectra of the sublimed **sBEHTDPP** (pink) and oCVD **pBEHTDPP** coating (green) prepared from BEHTDPP on glass substrates.

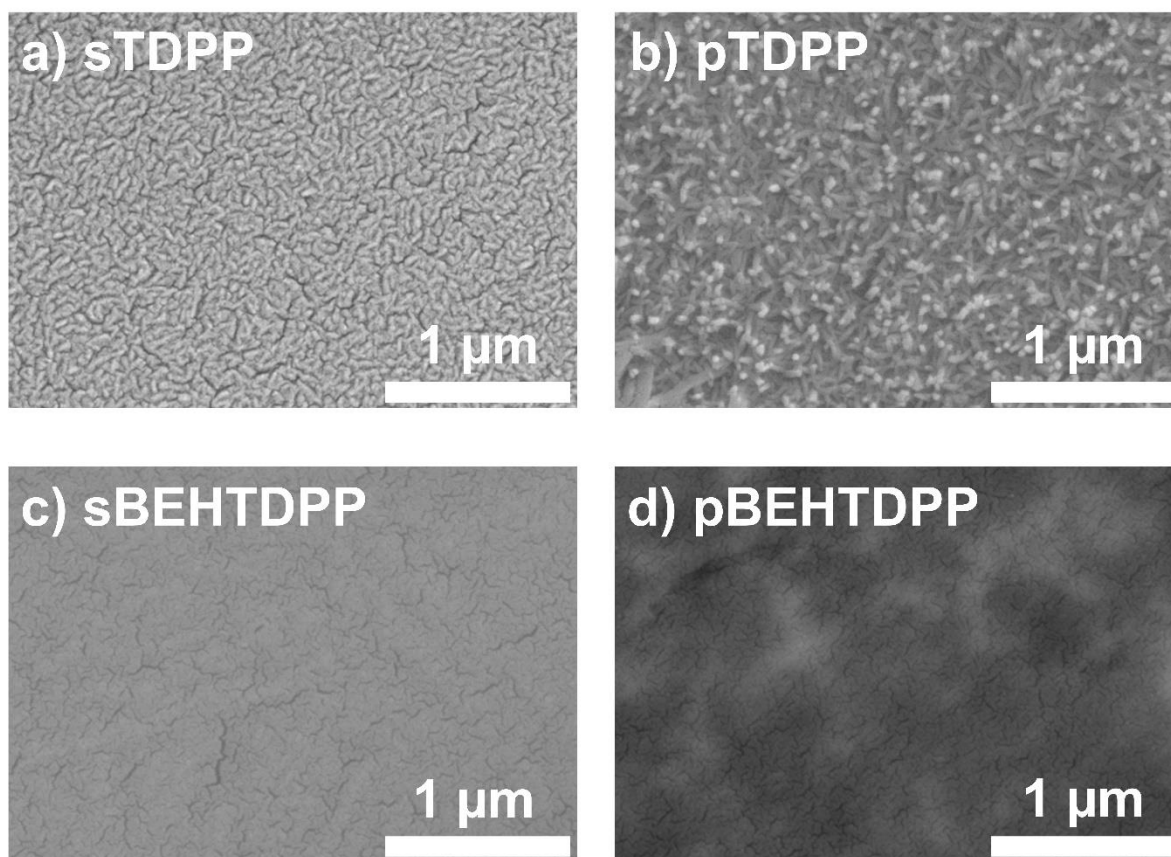


**Figure S6.** SEM images of the a) **sTDPP**, b) **pTDPP**, c) **sBEHTDPP** and d) **pBEHTDPP** samples prepared from the sublimation and oCVD reaction of TDPP and BEHTDPP, respectively.



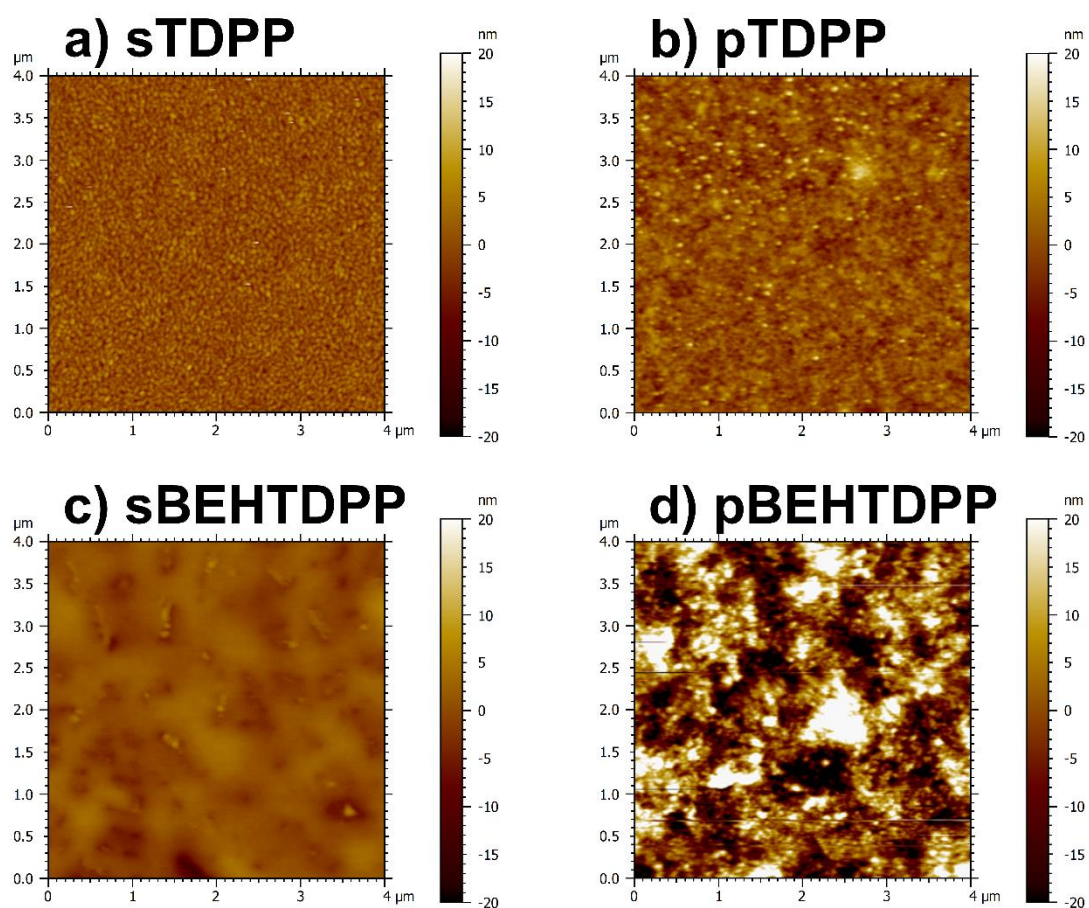


**Figure S7.** AFM topography images of the a) **sTDPP**, b) **pTDPP**, c) **sBEDTDPP** and d) **pBEDTDPP** samples prepared from the sublimation or oCVD reaction of TDPP and BEHTDPP, respectively. The same scale is used for the images to evidence differences in roughness between the coatings.

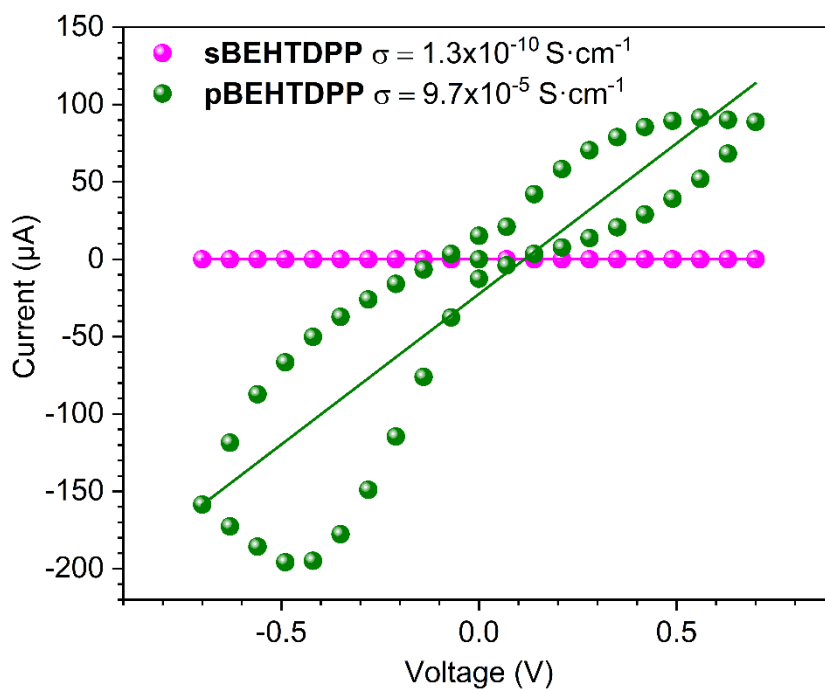


**Figure S8.** Lateral electrical conductivity measurement of sublimed **sBEHTDPP** coating (pink dots) and oCVD **pBEHTDPP** coating (green dots) on interdigitated chips. Pink and green solid lines show the linear fits used to determine the conductivities.

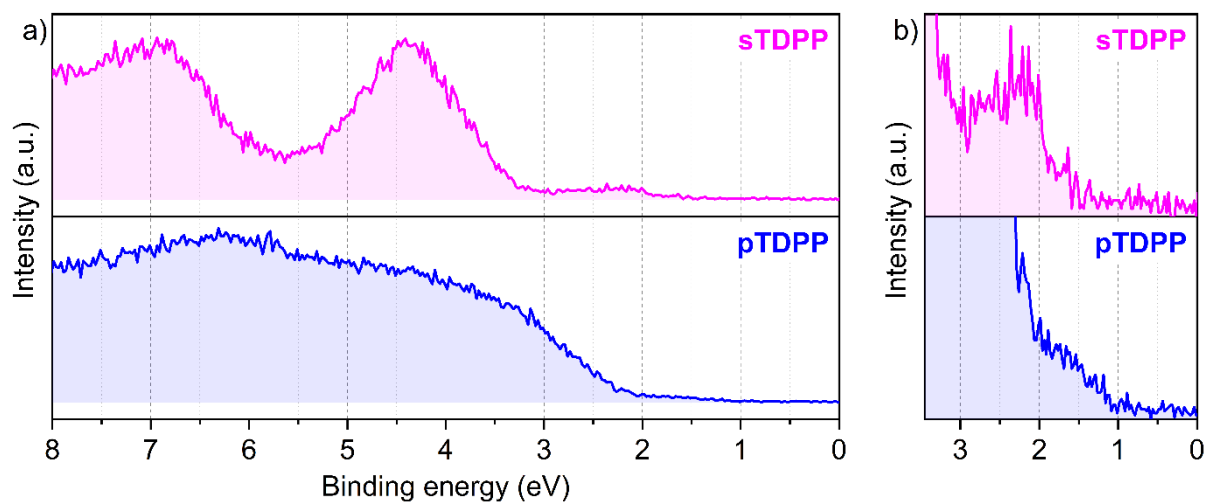


**Figure S9.** Valence band edge XPS spectra of the sublimed **sTDPP** and oCVD **pTDPP** coatings prepared from TDPP.

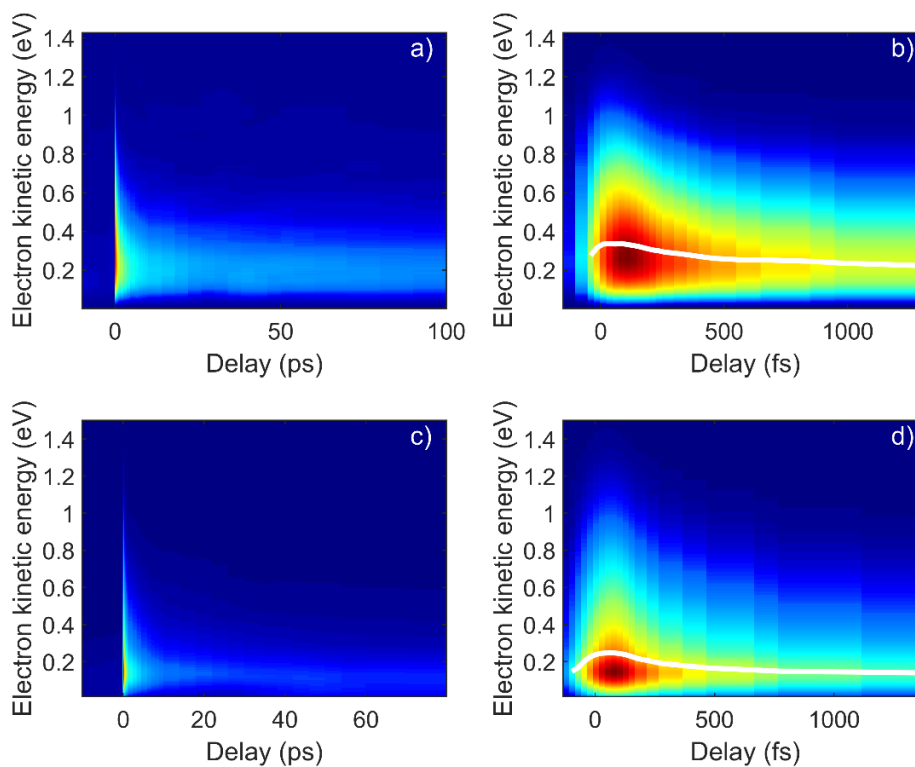


**Figure S10.** 2D representation of the 2PPE signals obtained for a-b) **pTDPP** and c-d) **pBEHTDPP**. b) and d) are zooms of a) and c), respectively. White lines correspond to the centre of mass for each delay.

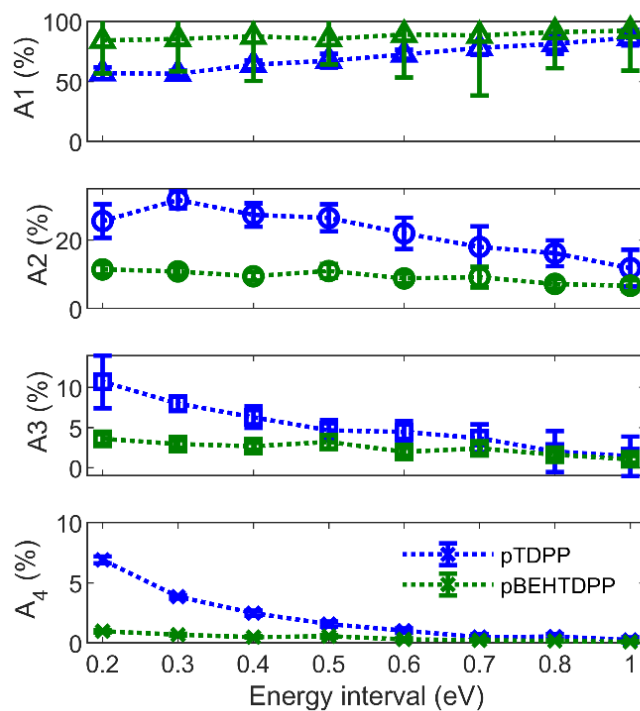


**Figure S11.** Relative amplitudes for the fitted tr-2PPE lifetimes.

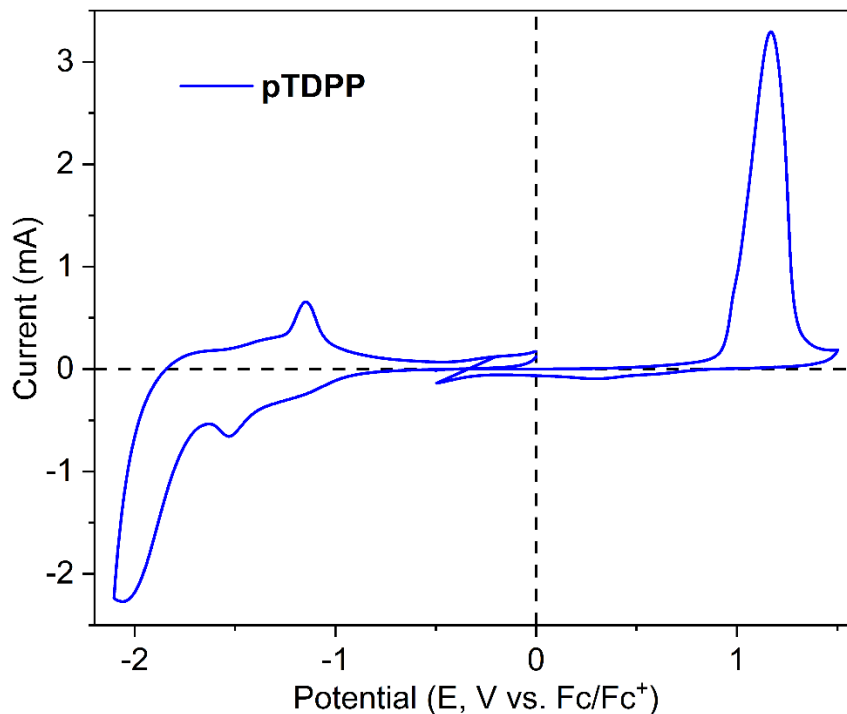


**Figure S12.** Anodic and cathodic cyclic voltammograms of **pTDPP** separately recorded at scan rate  $100 \text{ mV}\cdot\text{s}^{-1}$  in  $0.1 \text{ M Bu}_4\text{NPF}_6$  in  $\text{CH}_3\text{CN}$ . The anodic and cathodic scans were registered separately on fresh samples. In the range of positive potentials, an irreversible oxidation peak is observed with an onset potential of  $0.89 \text{ V}$  and a maximum potential reached at  $1.10 \text{ V vs. Fc/Fc}^+$ . These values are consistent with previous literature reports on electropolymerized N-alkylated (linear octyl and branched ethyl hexyl) thiophene-flanked DPPs.<sup>1</sup> The cathodic scan evidences a pair of redox peaks with an onset at  $-1.02 \text{ V}$  and maxima at  $-1.22 \text{ V}$  and  $-1.60 \text{ V}$ . Such values are significantly lower than the ones reported by Ponnappa *et al.*, i.e.  $-0.7 \text{ V}$  and  $-0.75 \text{ V}$ , for electropolymerized N-alkylated thiophene-flanked DPPs.<sup>1</sup> Such a shift of the cathodic peak might be explained by a longer conjugation length for the electrochemically synthesized polymers.

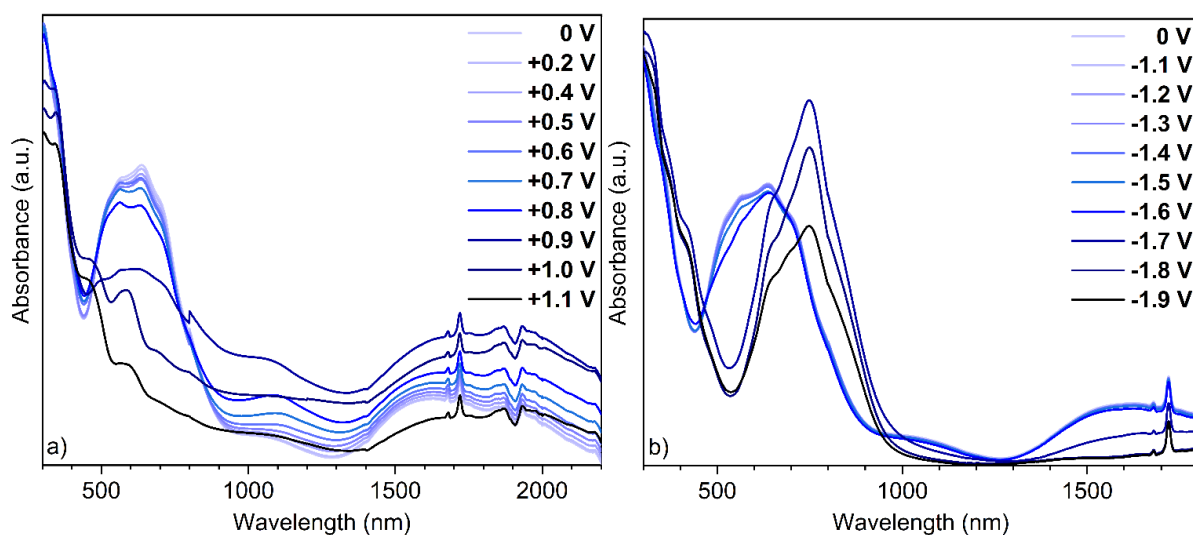


**Figure S13.** UV/Vis/NIR spectra of **pTDPP** on FTO registered at stepwise a) increasing and b) decreasing potentials in 0.1M Bu<sub>4</sub>NPF<sub>6</sub>/CH<sub>3</sub>CN. Potentials vs. Ag/Ag<sup>+</sup>. Upon increase of the working electrode potential, the intensity of  $\pi$ - $\pi^*$  transition band (at 637 nm) gradually decreases. Concomitantly, two broad absorption bands at ca. 1100 nm and ca. 1800 nm are observed to grow with increasing potential. These broad peaks are usually assigned to radical cations and di-cations generated in oxidized DPP-based conjugated oligomers<sup>2</sup> and polymers.<sup>3</sup> However, in comparison to previous works on N-alkylated TDPPs, these bands have relatively low intensities for **pTDPP**. This likely arises from a degradation process, whose occurrence at positive potentials is clearly evidenced by an irreversible oxidation peak on the CV curve (**Figure S12**). Particularly, above 0.8 V, the **pTDPP** coating is likely detached from the surface of the FTO-coated substrate, making impossible to record a spectrum of the fully oxidized form. In the range of negative potentials, the band at 637 nm, characteristic for the neutral polymer, also decreases upon changing of the potential from 0 V to -1.6 V. Jointly, a decrease of the absorbance in the NIR region is observed. For potentials of -1.7 V and beyond, a new and pronounced band is observed, with a maximum at 749 nm and with a shoulder at 835 nm. Such a behavior is consistent with the previous observations made for the reduction of DPP-based conjugated oligomers<sup>2</sup> and polymers,<sup>3</sup> and is attributed to formation of a radical anion. It must be mentioned, that in the present case, the reduction process is not correlated with an increase of absorption in the NIR region, which usually correlates with the presence of radical anions and dianions (or polaronic and bipolaronic states) in some reduced conjugated polymers.<sup>4</sup> Conversely, the band initially observed at higher wavelengths is shown to disappear likely due to removal of the residual positive charges generated during the oCVD process. For potentials beyond -1.9 V, the **pTDPP** coating is also detached from the FTO substrate.

## References

- 1 S. P. Ponnappa, S. Arumugam, S. Manzhos, J. MacLeod, H. J. Spratt, A. P. O'Mullane and P. Sonar, *J. Mater. Res.*, 2017, **32**, 2707–2718.
- 2 M. Gora, S. Pluczyk, P. Zassowski, W. Krzywiec, M. Zagorska, J. Mieczkowski, M. Lapkowski and A. Pron, *Synth. Met.*, 2016, **216**, 75–82.
- 3 M. Gora, W. Krzywiec, J. Mieczkowski, E. C. Rodrigues Maia, G. Louarn, M. Zagorska and A. Pron, *Electrochim. Acta*, 2014, **144**, 211–220.
- 4 R. Rybakiewicz-Sekita, P. Toman, R. Ganczarczyk, J. Drapala, P. Ledwon, M. Banasiewicz, L. Skorka, A. Matyjasiak, M. Zagorska and A. Pron, *J. Phys. Chem. B*, 2022, **126**, 4089–4105.